Supplementary Materials for

Monitoring cardiovascular disease severity using near-infrared mechanoluminescent materials as a built-in indicator

Xiangyu Liu,[a] Puxian Xiong,[b] Lejing Li,[c] Mei Yang,[d] Mingying Yang,*[d] and Chuanbin Mao*[a,e]

a. School of Materials Science and Engineering, Zhejiang University, Hangzhou, Zhejiang 310027, P. R. China
b. The State Key Laboratory of Luminescent Materials and Devices, Guangdong Provincial Key Laboratory of Fiber Laser Materials and Applied Techniques, School of Physics and Optoelectronics, South China University of Technology, Guangzhou 510640, P. R. China
c. The China-Germany Research Center for Photonic Materials and Devices, The State Key Laboratory of Luminescent Materials and Devices, Guangdong Provincial Key Laboratory of Fiber Laser Materials and Applied Techniques, School of Materials Science and Technology, South China University of Technology, Guangzhou 510640, P. R. China
d. Institute of Applied Bioresource Research, College of Animal Science, Zhejiang University, Yuhangtang Road 866, Hangzhou, Zhejiang 310058, P. R. China. E.mail: yangm@zju.edu.cn
e. Department of Chemistry and Biochemistry, University of Oklahoma, Norman, OK 73019, USA. E.mail: maophage@gmail.com

This file includes:

Materials and Methods

1. ML-AVGs Preparation

CaZnOS:Nd^{3+} MLPs were synthesized according to our reported protocol.[1] PDMS was used as the elastic base material to provide interior stress for the catheter (Fig. S1). First, 2 g of PDMS base resin and 1 g of MLPs (charged once by 254 nm UV light for 5 min) were mixed in a 1.5 mL centrifuge tube. Then, 0.2 g of hardener poly(dimethyl-methylhydrogenosiloxane)) were dispersed in the above mixture with constantly stirring. A stainless-steel wire with an outer diameter of 0.7 mm was chosen as the mold for catheter dipping. The mold was consistently immersed into and removed from the ML/PDMS complex solution at a constant rate for a total ten cycles. The dipping time for every mold in the ML/PDMS complex solution was 10 min. The curing time was 30 min at 60 °C. The layers wrapping the mold became the AVG, which was further cured at 80 °C for overnight. The resultant tubular ML-AVGs (4 mm × 1 mm) were removed from the mold and sterilized under UV lamp for 3 h and immersed into sterilized PBS for further experiments (Fig. S1).

2. Platelet Adhesion on ML Materials

Before the test, a standard curve was calculated using the solutions of known platelet concentrations. The rabbit whole blood was collected and placed into the sodium citrate-containing tubes and immediately centrifuged at 1500 rpm for 15 min. The platelet solution without erythrocytes was separated. The ML powders were compressed into disks for platelet adhesion. These disks were put into 24-well cell culture plate and immersed into normal saline (NS) solution for 2 h before being incubated with the platelet solution (PS). The NS solution was discarded and the platelet solution at a dose of 1 mL per well was added into the culture plate. The plate was subsequently placed at 37 °C in 5 % CO_2 for 1 h. After incubation, the ML disks were transferred into a new culture plate and rinsed 3 times with PBS to remove the unattached platelets. Subsequently, the disks were transferred into a lysis buffer to lyse the platelets adhered to the surface of disks and the lactate dehydrogenase (LDH) enzyme was quantified by enzyme-linked immunosorbent assay (ELISA) to evaluate the number of platelets. After that, the disks were placed into 4 % paraformaldehyde solution (PFA) at 4 °C for 2 h. After washing, dehydration with gradient ethanol and drying, the samples were prepared for electron microscopy imaging.[2]

3. Hemolysis of ML Materials

After sterilization, the ML powder samples were transferred into the centrifuge tubes and incubated with 5 mL of normal saline at 37 °C for 1 h. Rabbit whole blood (200 μL) was dispersed into each tube and incubated for another 1 h. Subsequently, the blood solutions were centrifuged at 800 rpm for 5 min and the absorbance of the supernatant at 540 nm

was measured. The hemolytic ratio (HR) was calculated by the formula: HR (%) = (AS - AN) / (AP - AN) × 100. AS represented the absorbance value of the ML samples group. AP represented the absorbance value of the positive control group (5 mL ultra-pure water with 200 μL whole blood). AN represented the absorbance value of the negative control group (5 mL physiological saline with 200 μL whole blood).

4. Subcutaneous Implantation of ML Materials

Adult Balb/c mice (20-22 g, male) were used to evaluate the histocompatibility of the ML materials. For surgery, the mice were anesthetized, and ML powder was mixed with 0.9 % normal saline (5 mg sample per 100 μL) and injected into subcutaneous tissue on the back. In each group, the mice were sacrificed after 1 day, 7 days, 14 days and 28 days, and the subcutaneous tissues and major organs (kidney, lung, heart, spleen and liver) were collected and immersed in 4 % PFA for 12 h at 4 °C for paraffin section for Hematoxylin & Eosin (H&E) staining, Masson's trichrome staining, immunofluorescence staining of macrophage, and proinflammatory cytokine and chemokine measurements by ELISA. The immunofluorescence staining was performed as follows: after antigen heat retrieval, the sections were washed using PBS and blocked using 5 % BSA containing 0.1 % Triton X-100. Rabbit anti-CD68 (M1 macrophage marker, Cat. #: 28058-1-AP, Proteintech) and rabbit anti-CD163 (M2 macrophage marker, Cat. #: 16646-1-AP, Proteintech) were used as the primary antibodies. The sections were incubated with the primary antibodies at 4 °C for 12 h followed by incubation with the secondary antibody (donkey anti-rabbit, 1:300) for 30 min at 37 °C. Cell nuclei were stained using DAPI. The animal study was approved by the Institutional Animal Care and Use Committee of Zhejiang University.

The evaluation of CD68 and CD163 was performed on the wound center area as previously described.[3] Briefly, five regions of interest (ROIs) of 0.3 mm^2 were randomly chosen from each wound sample to calculate the positive fluorescent area using a pixel threshold on 8-bit converted images using Image J software and expressed as the area fraction of positive signal per ROI. The data points from five ROIs were averaged and expressed as the average area fraction of positive fluorescent signal per mouse. Each data point of CD68 and CD163 in the figures in the main text represented an average area fraction of an animal. In the analysis of immunohistochemistry, the researchers were blinded to the ROI selection and quantitative calculation.

5. CCA Implantation Surgery

Adult Sprague-Dawley rats were used to evaluate the monitoring effect of ML materials. Rats were anesthetized using isoflurane, and the furs on the ventral neck and temporal region were shaved and disinfected using povidone iodine and 75 % ethanol swabs. The sterile gauze was spread on the surgical site. A 1.5 cm central midline incision was made

on the exposed neck. The muscles and glands were gently moved laterally to the trachea on both sides. The arteries were dissected from surrounding fascia and the arterial sheath was stripped from the arteries. The CCA, external carotid artery (ECA) and internal carotid artery (ICA) were then exposed. Caution should be made to avoid the damage of the vagus nerves near CCA which could otherwise result in respiratory failure. ECA was ligated using silk sutures, and CCA and ICA were temporarily closed using artery clamps. A 0.3 mm tiny incision was made on the ECA, and then the ML-AVG catheter was inserted through ECA into CCA. Then the tiny incision on the ECA was ligated using silk sutures and the artery clamps were removed to recover blood flow through the ML-AVG catheter (Fig. S10). The diameter of the CCA was adjusted to simulate the vascular occlusion as follows: The CCA was exposed and a silk suture was gently applied around the outer wall of the CCA. Then, the silk suture was marked and cut at the knot point. The length of the interception of the silk suture was measured to determine the circumference of the CCA. The diameter of CCA was calculated. The circumferences corresponding to one third and two third diameters were also calculated and the lengths were marked on the silk suture. We used the silk suture to shrink CCA to control the degrees of opening of CCA to represent different degrees of vascular occlusion (0/3 means that the inner diameter of CCA is completely closed; 1/3 means that the CCA is opened one third; 2/3 means that the CCA is opened two thirds; 3/3 means that the CCA is completely opened, which is the normal status of CCA) (Fig. S15). Different doses of adrenaline (10, 20 and 40 mg/kg) were injected into rats to temporarily increase the blood pressure for simulating hypertension. The blood pressure, systolic pressure, and diastolic pressure were tested using a MP150 physiological signal recording and analysis system (BIOPAC Systems, Inc). Rats were anesthetized using isoflurane, and the furs on the ventral neck region were shaved and disinfected using povidone iodine and 75 % ethanol swabs. A 3 cm central midline incision was made on the exposed neck. The CCA was exposed and temporarily closed using artery clamps. A catheter connected with a pressure sensor and the MP150 physiological signal recording and analysis system was inserted into the CCA and fixed. The artery clamps were removed from the CCA and the blood pressure, systolic pressure, and diastolic pressure were recorded. The mean arterial pressure was calculated by the following formula: mean arterial pressure (mmHg) = (systolic pressure - diastolic pressure)/3 + diastolic pressure. The state of the ML-AVGs implanted in the CCA was monitored using a combination of the thermal camera, NIR spectrometer and NIR camera (Fig. 1A). After ML-AVGs were implanted into the CCA of rat, the thermal camera was fixed directly above the CCA. Excess blood and tissue exudate were cleaned up and 3 ml of normal saline was added on the surface of wound to infiltrate the tissue. The pictures of the neck of rats were captured by the thermal camera, and the optical signals of ML-AVGs in CCA in the pictures were converted to grayscales and the values of grayscale were calculated by image J. The blank PDMS graft was used as the control group. The relative NIR signal intensity of ML/PDMS graft was obtained by subtracting the grayscale value of the control group from the original grayscale value

of the ML/PDMS graft.

6. Blood Compatibility Test of ML-AVGs In Vivo

Adult Sprague-Dawley rats (280-300 g, male) were used to evaluate the blood compatibility of ML-AVGs in vivo. The rats were randomly divided into 2 groups after ML-AVGs were implanted into the CCA. One group of rats received subcutaneous injection of heparin solution (200 U/kg per day) for 30 consecutive days after ML-AVGs surgery (the heparin treatment group), the other group of rats were injected subcutaneously with heparin just for 2 days after surgery (the non-heparin treatment group). The rats were sacrificed and the blood vessels contained ML-AVGs were removed from the CCA 1, 7, 14, 30, and 60 days after implantation, respectively. The blood vessels were infused with 2.5 % glutaraldehyde solution at 4 °C for 2 h. The ML-AVGs were removed from the blood vessels and washed three times using ultrapure water and dehydrated using gradient concentration of ethanol solution, then the samples were placed in a vacuum drying oven for 2 days. Before SEM test, the ML-AVGs were evenly cut lengthwise in half and the inner surface of ML-AVGs was used to photograph and analyze the blood compatibility of materials in vivo.

7. Statistics

IBM SPSS Statistics 19.0 and GraphPad Prism 7 were used to perform statistical analysis. Data are presented as mean ± SEM. Differences among groups were calculated using one-way ANOVA with Student’s t-test.

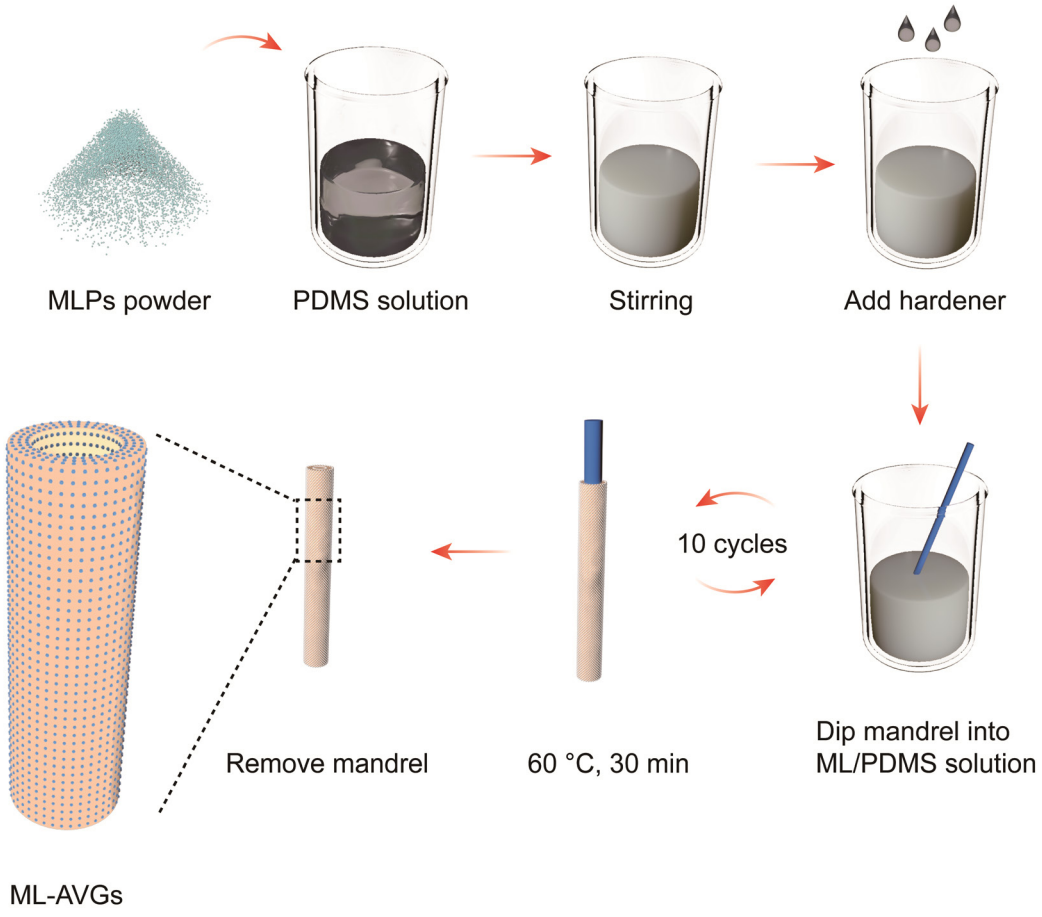

Fig. S1. The Schematic diagram of preparation procedures of ML-AVGs. MLPs: Mechanoluminescence particles; PDMS: Polydimethylsiloxane;

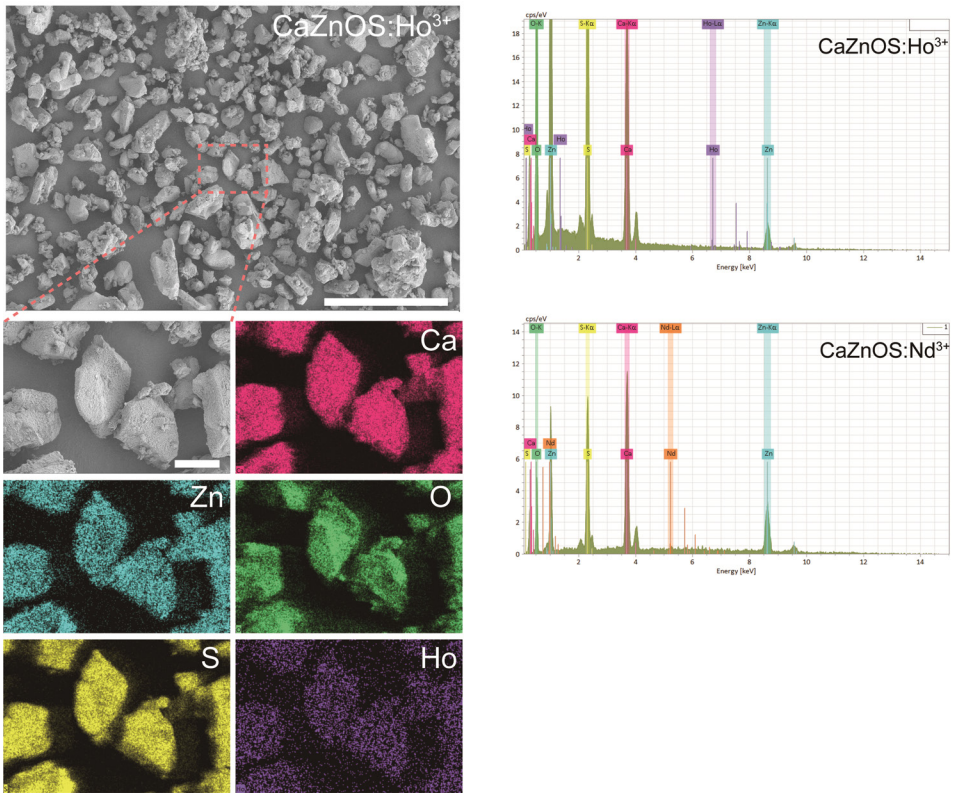

Fig. S2. SEM images and Energy Dispersive Spectrometer (EDS) analysis of $CaZnOS:Ho^{3+}$ and $CaZnOS:Nd^{3+}$ particles. Scale bars represent 100 µm (up) and 15 µm (bottom).

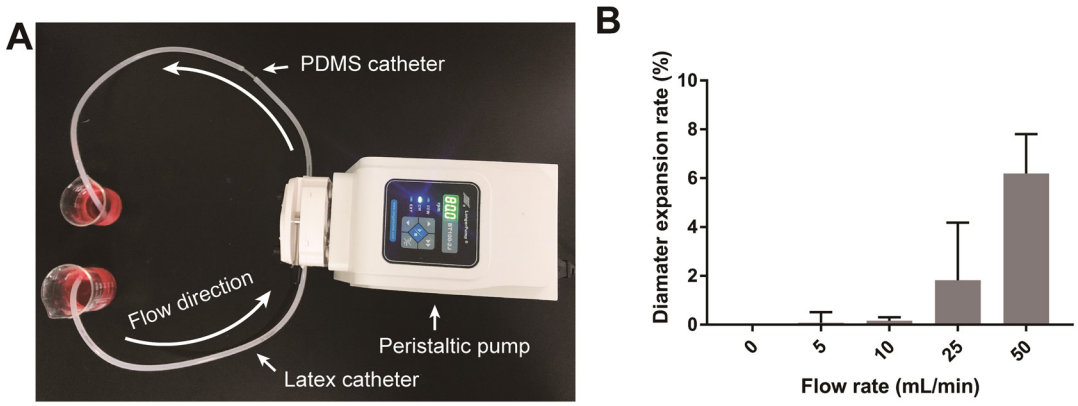

Fig. S3. The role of flow rate on PDMS stretching. (A) The test strategy for studying the effect of flow rate on the PDMS AVGs stretching. (B) The PDMS AVGs stretching under different flow rates.

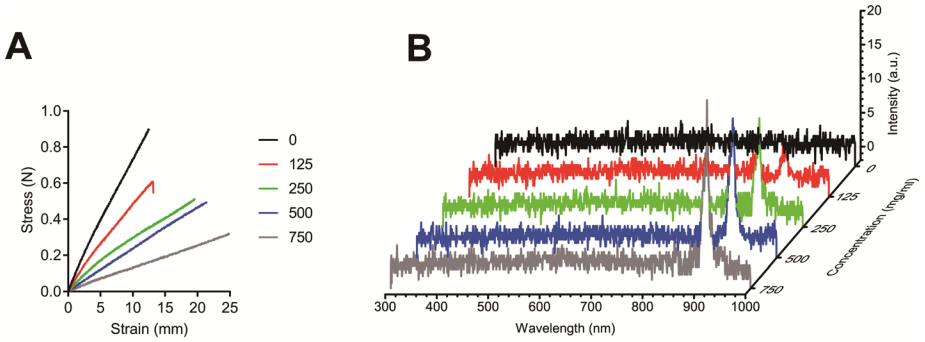

Fig. S4. Mechanical properties and emission spectra of ML-AVGs with different MLPs concentrations. (A) Mechanical properties of ML-AVGs with 0, 125, 250, 500, and 750 mg/ml of MLPs. (B) Emission spectra of ML-AVGs with 0, 125, 250, 500, and 750 mg/ml of MLPs under 24 kPa pressure.

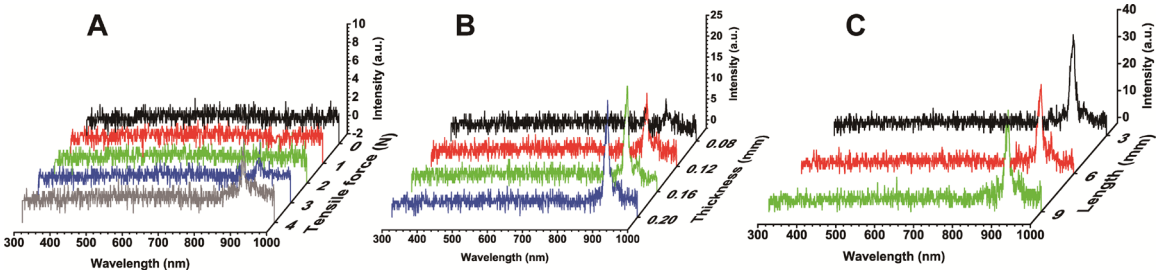

Fig. S5. The emission spectra of ML-AVGs under different (A) tensile forces, (B) wall thicknesses, and (C) lengths.

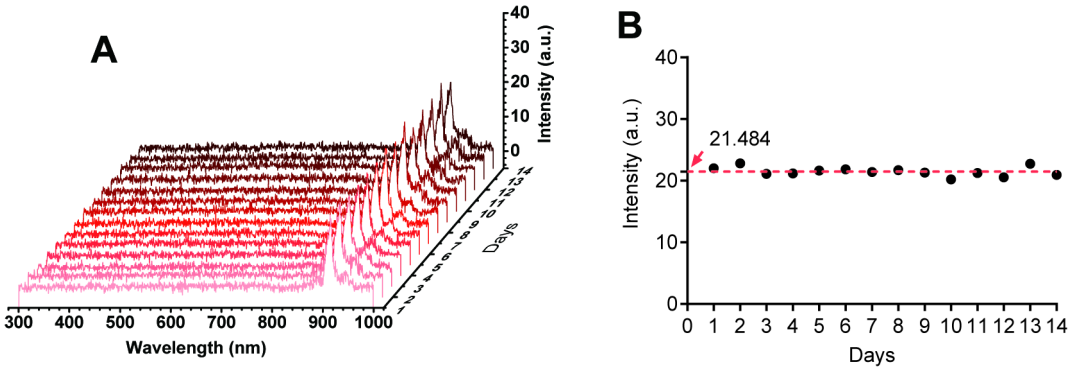

Fig. S6. The temporal reliability of the material in vitro.

(A) The emission spectra and (B) the signal intensity at 908 nm of ML-AVGs under cyclic loading (24 kPa) over 14 days.

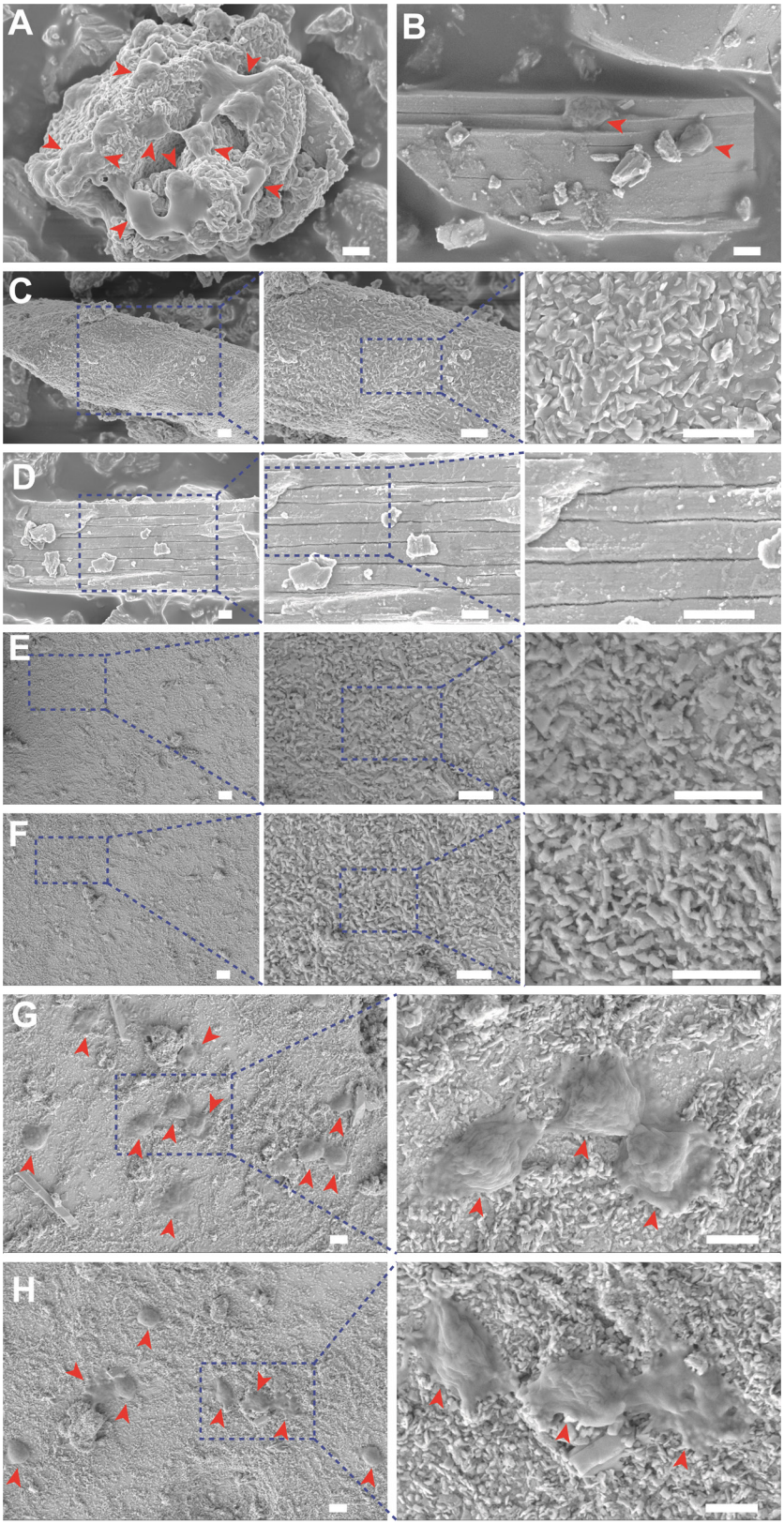

Fig. S7. In vitro platelet adhesion on ML materials. (A, B) The platelet adhesion test

on (A) CaZnOS:Ho^{3+} particles and (B) CaZnOS:Nd^{3+} particles. Scale bars represent 1 μm. (C, D) The microscopic morphology of (C) CaZnOS:Ho^{3+} particles and (D) CaZnOS:Nd^{3+} particles. Scale bars represent 1 μm. (E, F) The microscopic morphology of (E) CaZnOS:Ho^{3+} and (F) CaZnOS:Nd^{3+} nanoparticles formed by crushing the big ML particles. Scale bars represent 1 μm. (G, H) The platelet adhesion test on the surface with deposited (G) CaZnOS:Ho^{3+} nanoparticles and (H) CaZnOS:Nd^{3+} nanoparticles. Scale bars represent 1 μm. Red arrows indicate platelets.

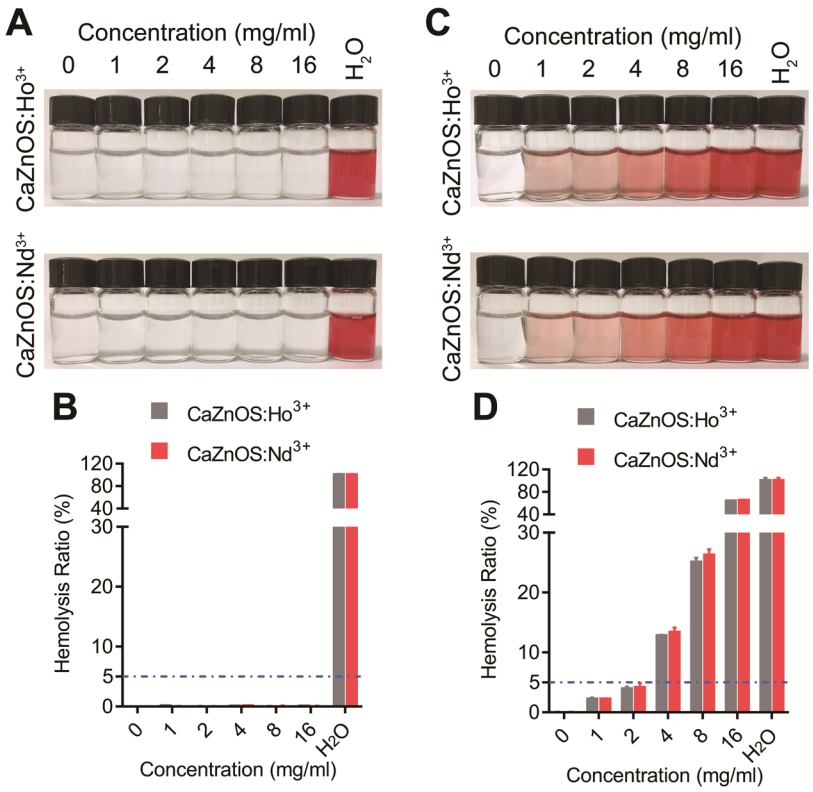

Fig. S8. In vitro hemolysis tests on ML materials. (A) Digital photographs of hemolysis effects and (B) hemolysis ratio of the supernatant of ML materials in normal saline. (C) Digital photographs of hemolysis effects and (D) hemolysis ratio of ML nanoparticles. *$p < 0.05$, **$p < 0.005$ and ***$p < 0.0005$, analyzed by one-way ANOVA with Student's t-test, n=5.

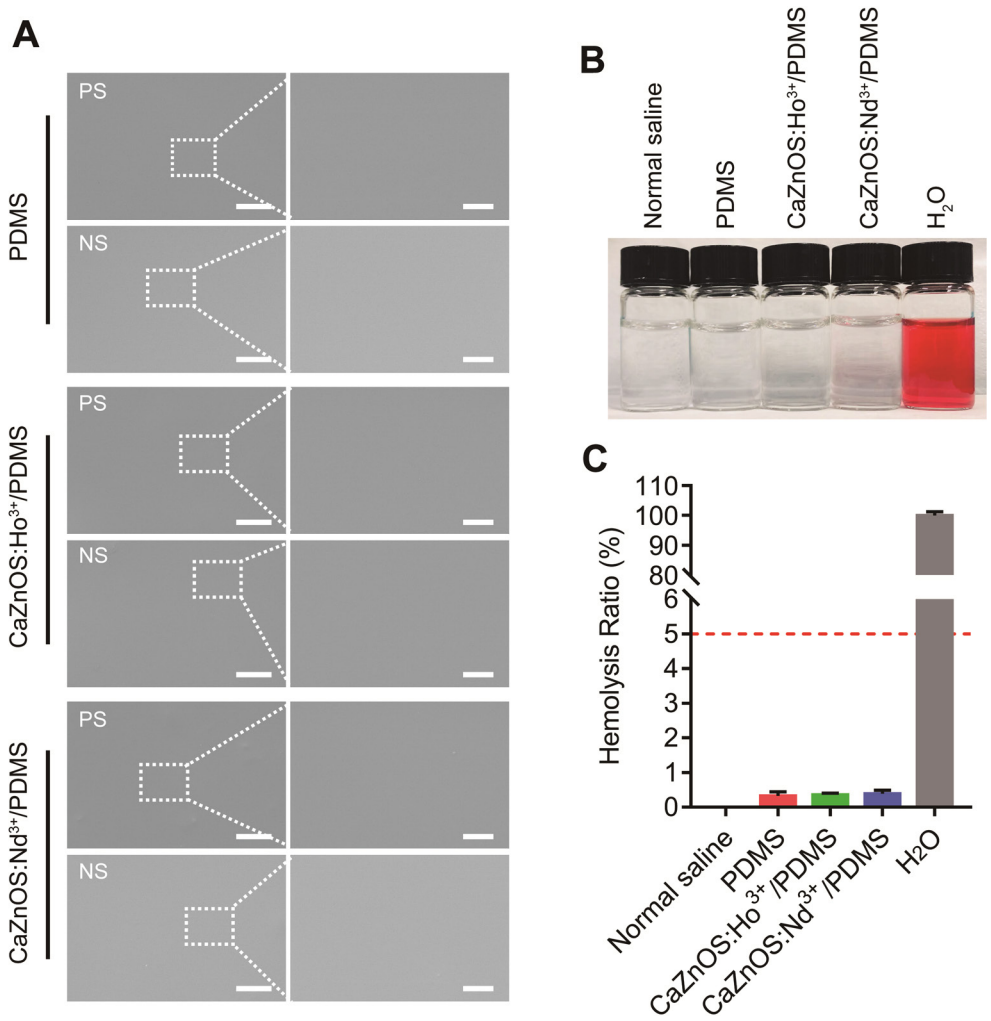

Fig. S9. In vitro blood compatibility of the ML/PDMS composite materials. (A) Scanning electron microscope photographs of platelets adhered onto the ML/PDMS disks after ML/PDMS disks were incubated with the platelet solution (PS) and normal saline (NS). Scale bars represent 5 μm (left) and 1 μm (right). (B) Digital photographs of hemolysis effects and (C) hemolysis ratio. *$p < 0.05$, **$p < 0.005$ and ***$p < 0.0005$, analyzed by one-way ANOVA with Student's t-test, n=5.

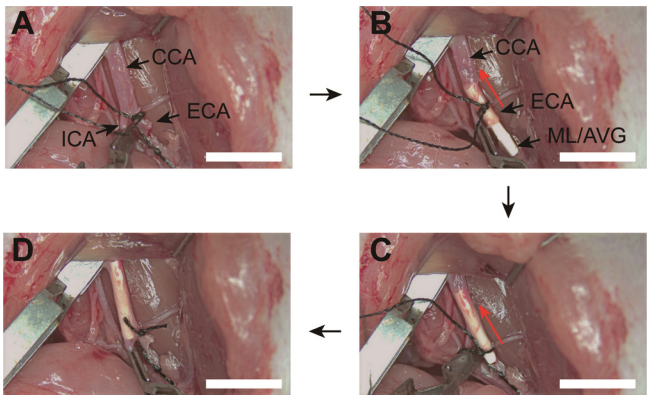

Fig. S10. Surgical procedure for ML-AVG insertion. (A) Ligature of ECA using silk suture; Closure of CCA and ICA using artery clamps; Formation of a 0.3 mm tiny incision on the ECA. (B, C) Insertion of the ML/AVGs through ECA into CCA. (D) Ligature of the tiny incision on the ECA using silk stature. Scale bars represent 5 mm.

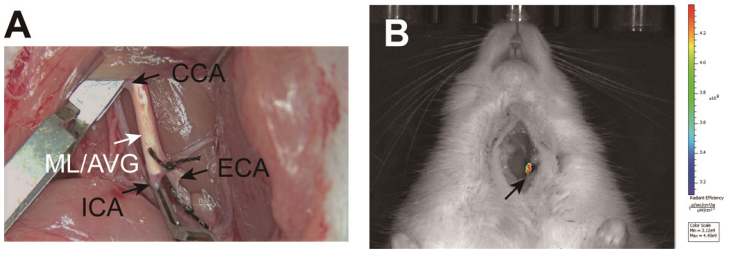

Fig. S11. Images of ML-AVGs in CCA. (A) The digital image of ML-AVG in the CCA. (B) The live animal imaging of ML-AVGs after the grafts were inserted into the CCA of the rats. The fluorescein FITC was added into the PDMS solution during the procedure of ML-AVGs preparation. The emission light at 525 nm could be emitted from the ML-AVGs containing FITC under the excitation light at 490 nm.

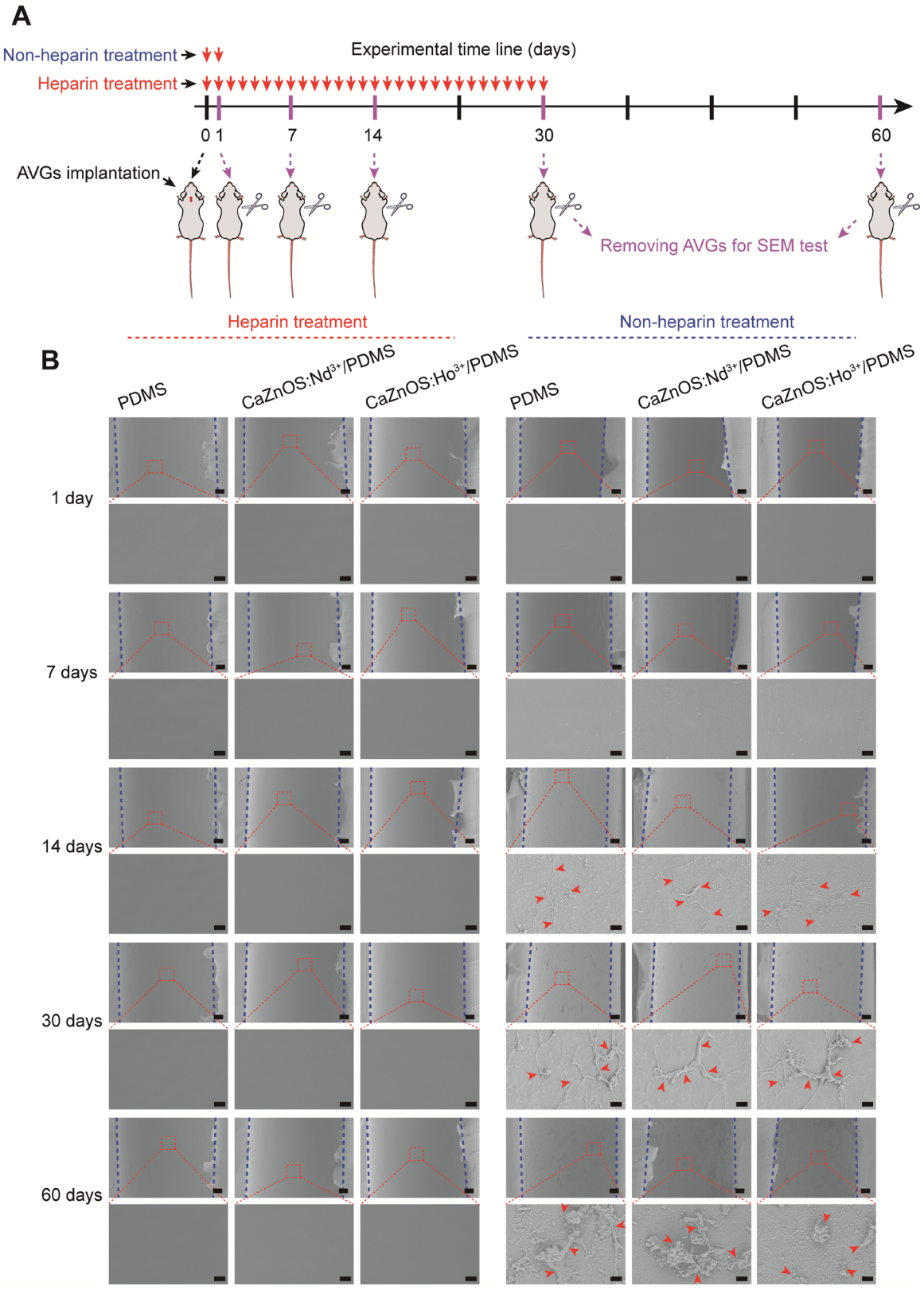

Fig. S12. The in vivo blood compatibility of ML-AVGs. (A) The experimental time line.

To evaluate the blood compatibility of AVGs (PDMS, CaZnOS:Nd^{3+}/PDMS, and CaZnOS:Ho^{3+}/PDMS) in vivo, the AVGs were implanted into common carotid artery (CCA) of rats. One group of rats after surgery were injected subcutaneously with heparin (red arrows) for 30 days (the heparin treatment group), the other group of rats were injected subcutaneously with heparin just for 2 days (the non-heparin treatment group). The AVGs were removed from CCA for scanning electron microscope (SEM) test 1, 7, 14, 30, and 60 days after implantation, respectively. (B) SEM images of the internal surface of AVGs removed from CCA 1, 7, 14, 30, and 60 days post implantation. Blue dotted lines showed the boundary of the internal surface of AVGs. n=3 mice per time point. Scale bars represent 20 μm (top) and 2 μm (bottom).

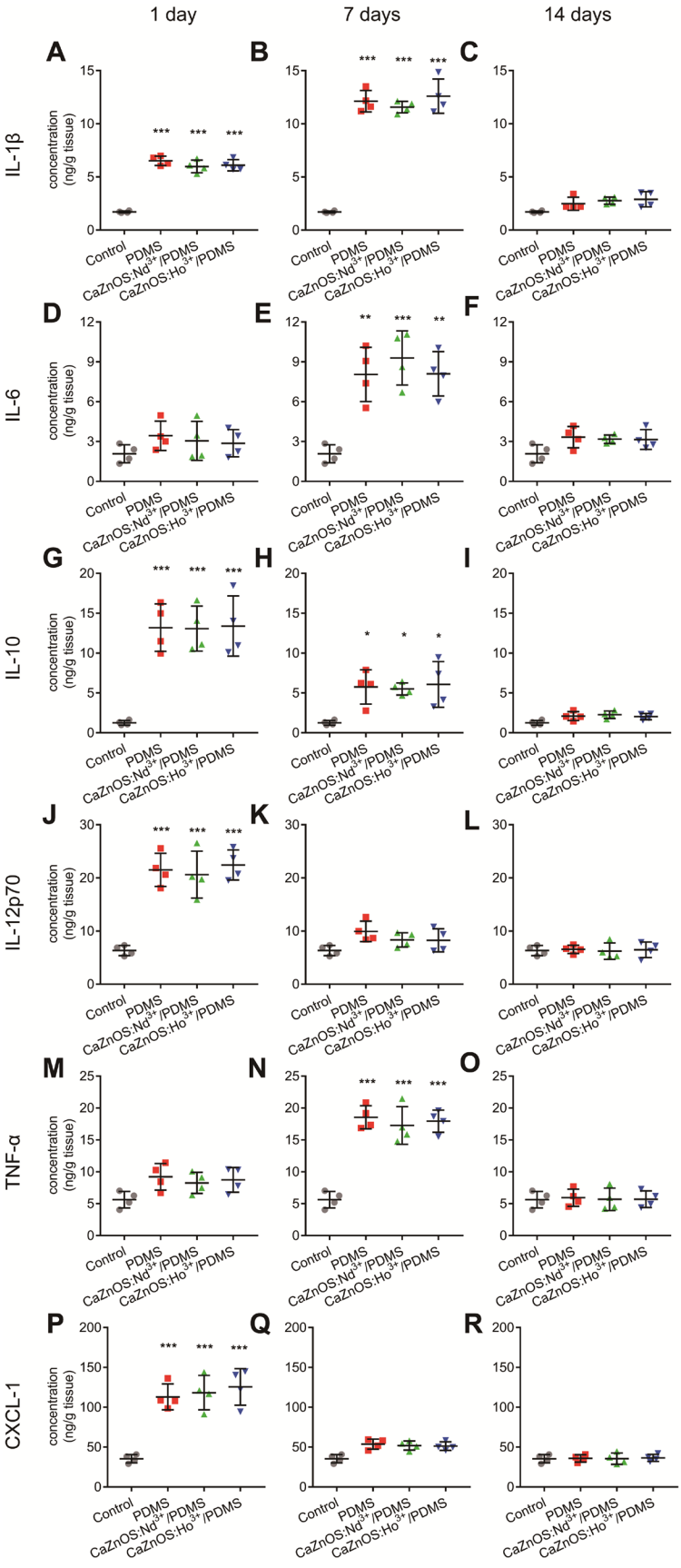
1 day
7 days
14 days
IL-1β
IL-6
IL-10
IL-12p70
TNF-α
CXCL-1
concentration (ng/g tissue)
Control
PDMS
CaZnOS:Nd3+/PDMS
CaZnOS:Ho3+/PDMS

Fig. S13. The proinflammatory response elicited by the control (gray), PDMS (red), CaZnOS:Nd^{3+}/PDMS (green) or CaZnOS:Ho^{3+}/PDMS (blue) 1 day, 7 days, and 14 days post subcutaneous implantation. The peri-implant concentrations of (A-C) IL-1β, (D-F) IL-6, (G-I) IL-10, (J-L) IL-12p70, (M-O) TNF-α, and (P-R) CXCL-1. n = 4 mice per time per group point. Data points represent mean ± s.e.m. for ng/g tissue, *$p < 0.05$, **$p < 0.005$, ***$p < 0.0005$, analyzed by one-way ANOVA with Student's t-test.

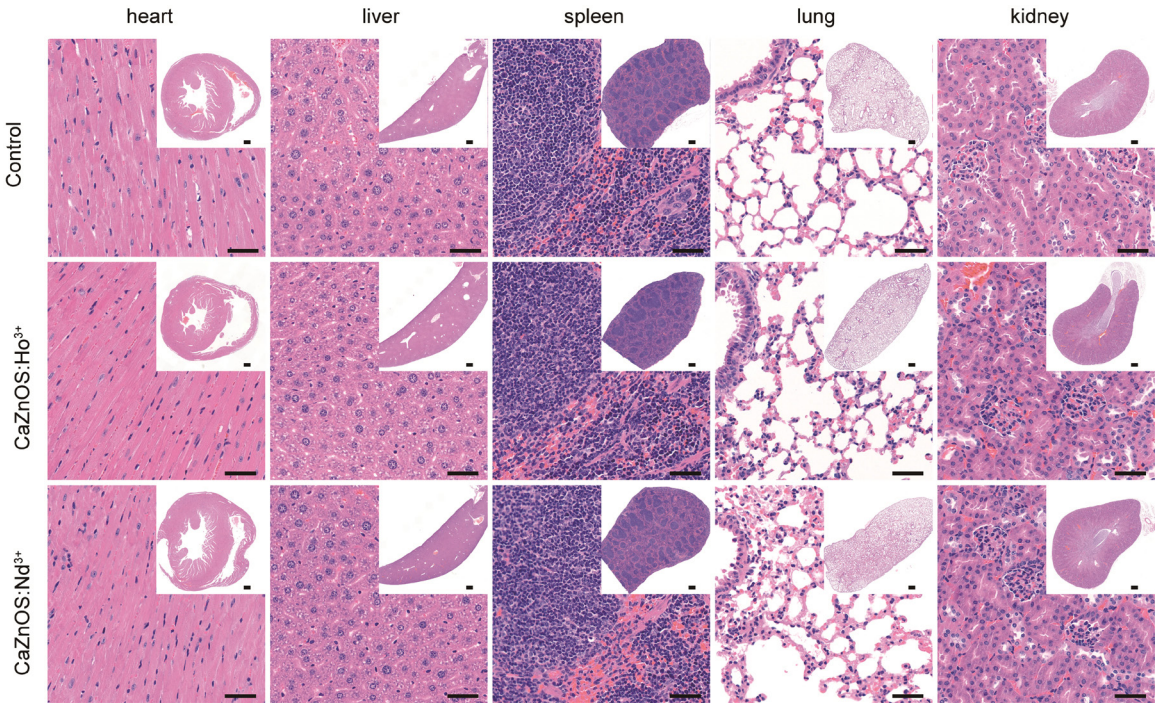

Fig. S14. Histological analysis of major organs collected from the blank control, CaZnOS:Ho^{3+} and CaZnOS:Nd^{3+} after 4 weeks implantation. Scale bars represent 50 μm (high magnification) and 500 μm (low magnification).

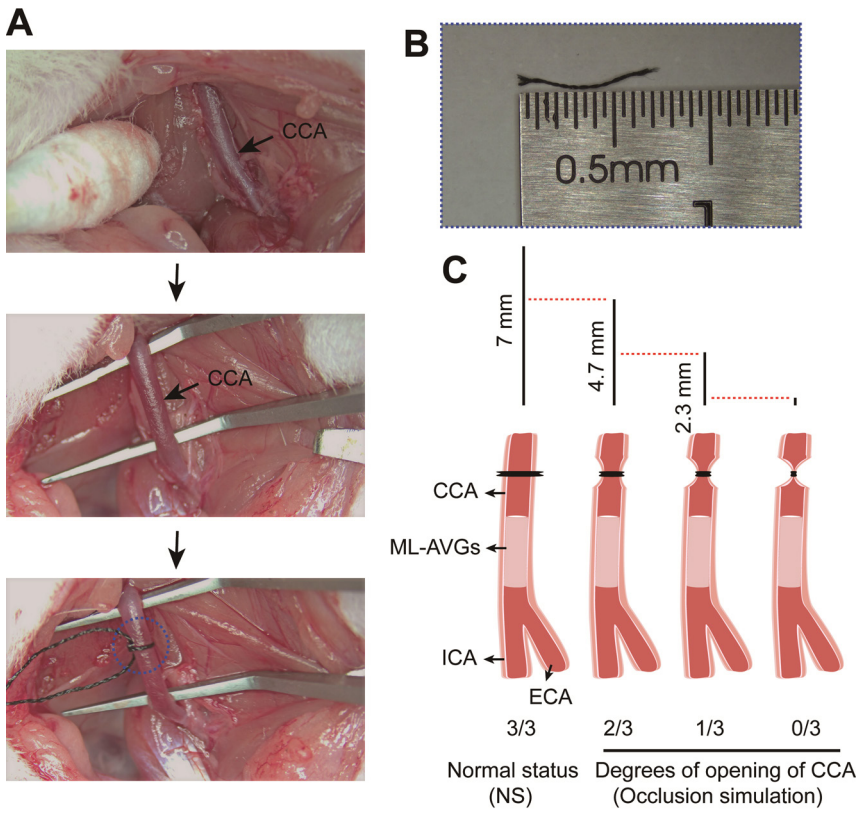

Fig. S15. The method of narrowing the CCA. (A) The CCA was exposed and a silk suture was gently applied around the outer wall of the CCA. (B) the silk suture was cut and the length of the silk suture was measured to determine the circumference of the CCA. (C) The schematic diagram of adjusting the CCA diameters by tightening the silk suture to varying degrees.

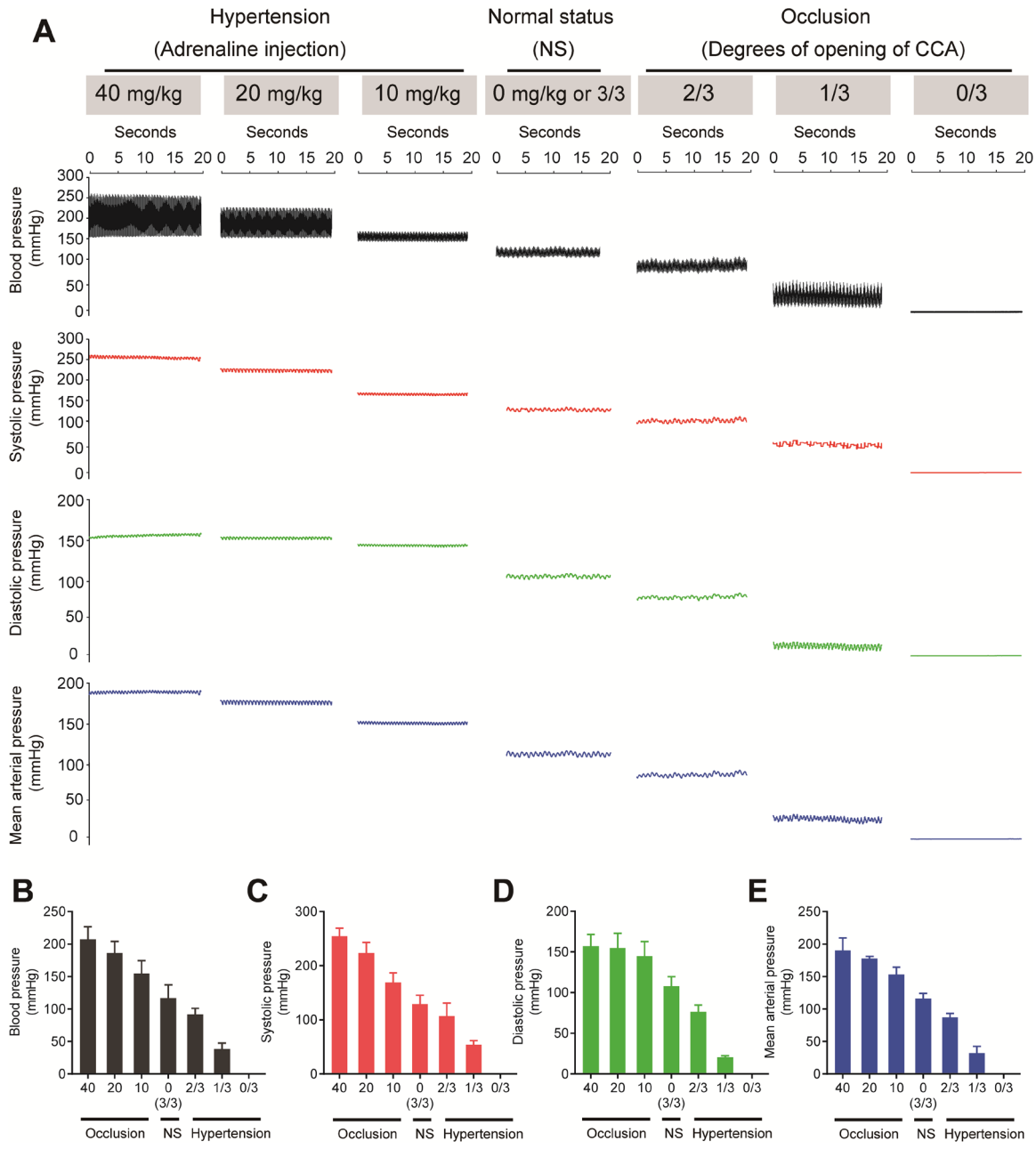

Fig. S16. The blood pressure study of CCA under adrenaline administration and different degrees of opening of CCA. (A) The signal line of blood pressure, systolic pressure, diastolic pressure and mean arterial pressure. (B-E) The histogram of (B) blood pressure, (C) systolic pressure, (D) diastolic pressure, and (E) mean arterial pressure. n=4 rats per group.

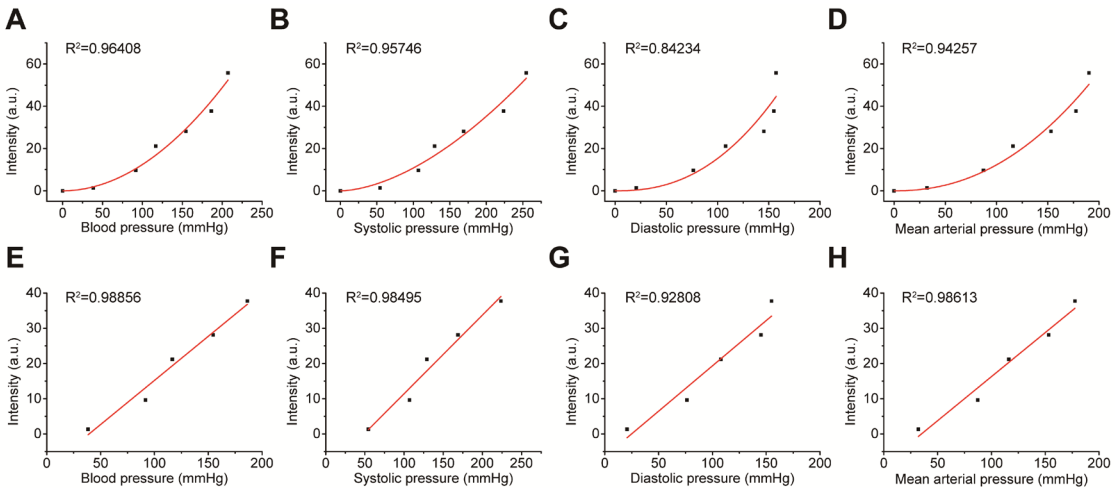

Fig. S17. The standard curve between luminescent signal intensity and different blood pressure. (A-D) The non-linear curve between the signal intensity and (A) blood pressure (0 - 207.27 mmHg), (B) systolic pressure (0 - 254.83 mmHg), (C) diastolic pressure (0 - 157.14 mmHg), and (D) mean arterial pressure (0 - 190.12 mmHg). (E-H) The linear curve between signal intensity and (E) blood pressure (38.44 - 186.43 mmHg), (F) systolic pressure (54.47 to 223.7 mmHg), (G) diastolic pressure (20.66 to 154.9 mmHg), and (H) mean arterial pressure (32.09 - 177.62 mmHg).

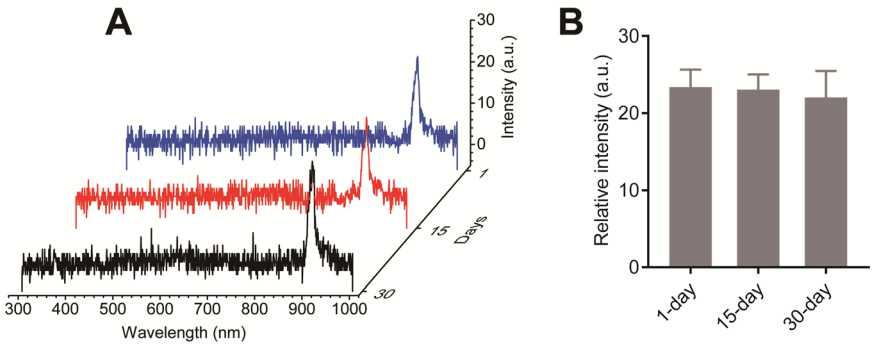

Fig. S18. The temporal reliability of the ML-AVGs in vivo. (A) The emission spectra and (B) signal intensity at 908 nm of ML-AVGs over 30 days in vivo.

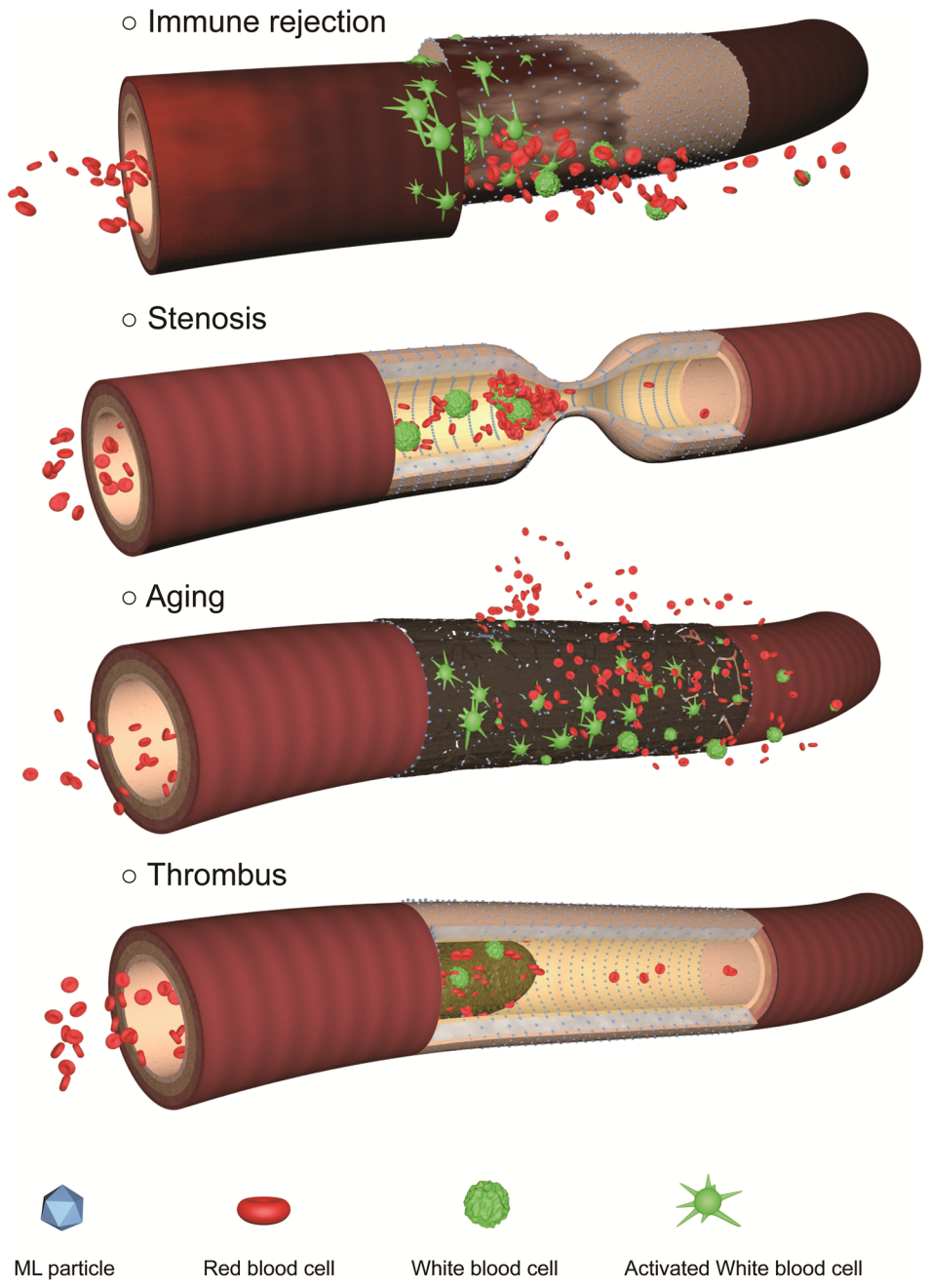

Fig. S19. Typical failures of AVGs in vivo and aspects of mechanoluminescent (ML) materials that can be applied in the vascular grafts.

1. L. Li, L. Wondraczek, Y. Zhang, Y. Zhu, M. Peng and C. Mao, *ACS Appl. Mater. Interfaces*, 2018, **10**, 14509-14516.
2. X. Y. Liu, Y. Q. Niu, K. C. Chen and S. G. Chen, *Mater. Sci. Eng. C-Mater. Biol. Appl.*, 2017, **71**, 289-297.
3. S. R. Li, L. R. Nih, H. Bachman, P. Fei, Y. L. Li, E. Nam, R. Dimatteo, S. T. Carmichael, T. H. Barker and T. Segura, *Nat. Mater.*, 2017, **16**, 953-961.